J Toxicol Pathol 2015; 28: 237–241

Case Report

Spontaneous early-onset glomerulonephritis in a 8-week-old male Crj:CD1 (ICR) mouse

Kyohei Ago[1*], Go Sugahara[2], Kinji Shirota[2, 3], and Yasushi Kurata[1]

[1]Toxicology Laboratory, Pharmaceutical Research Center, Meiji Seika Pharma Co., Ltd., 760 Morooka-cho, Kohoku-ku, Yokohama, Kanagawa 222-8567, Japan
[2]Research Institute of Biosciences, Azabu University, 1-17-71 Fuchinobe, Sagamihara, Kanagawa 229-8501, Japan
[3]Laboratory of Veterinary Pathology, Azabu University, 1-17-71 Fuchinobe, Sagamihara, Kanagawa 229-8501, Japan

Abstract: Glomerular lesions including membranoproliferative glomerulonephritis occur spontaneously in aged mice, but they are rare in young animals. In our laboratory, spontaneous glomerulonephritis was observed in an 8-week-old male Crj:CD1 (ICR) mouse. Macroscopically, the bilateral kidneys were discolored, but no edema or ascites was observed. Glomerular lesions were characterized by a thickening of capillary walls, a double-contoured basement membrane and mesangial expansion due to increased amounts of matrix. Ultrastructurally, mesangial interposition in the capillary wall and subendothelial deposition of basement membrane-like material were observed. No evidence of immune complex deposition or amyloid was found. On the basis of the observed clinical pathology and histopathology, a secondary form of glomerular lesion was excluded. The glomerular lesion was compatible with glomerulonephritis in a young Crj:CD1 (ICR) mouse. (DOI: 10.1293/tox.2015-0015; J Toxicol Pathol 2015; 28: 237–241)

Key words: glomerulonephritis, spontaneous, kidney, mouse, CD-1

Glomerular lesions have been reported in aged rodents including glomerulonephritis[1], hyaline glomerulopathy[2], amyloidosis[3], mesangioproliferative glomerulopathy[4] and glomerulosclerosis[3]. In addition, mice with complement factor H (CFH)-deficient membranoproliferative glomerulonephritis[5] or cryoglobulinemic glomerulonephritis[6] and rats with Heymann nephritis[7] are used as animal models of glomerular lesions. However, the cause and pathogenesis of spontaneous glomerular lesions have not been completely elucidated, and therefore, it is unclear whether these lesions are involved in the pathogenesis of these animal models. We found a case of glomerulonephritis in a young 8-week-old Crj:CD1 (ICR) mouse. This study characterized the morphological and immunohistochemical features of this case of glomerulonephritis.

This study was conducted in compliance with the "Guidelines for Management of Animal Experiments" established by Meiji Seika Pharma Co., Ltd., using a procedure approved by the Animal Care and Use Committee. Eight-week-old male ICR [Crj:CD1 (ICR)] mice (n = 51) had been purchased from Charles River Laboratories Japan (Hino, Japan) for a pharmacological study and housed in aluminum cages with five animals per cage. The animals were allowed *ad libitum* access to tap water adjusted to a chloride concentration of approximately 2 ppm and a commercial solid basal diet (CRF-1, Oriental Yeast Co., Ltd., Tokyo, Japan). The animal room was maintained at a temperature of 23 ± 2°C, humidity of 55 ± 10% and lighting for 12 hours.

During the quarantine and acclimatization period, one mouse showed a decrease in body weight. Three days after the beginning of the quarantine period, the mouse was sacrificed for necropsy. Under isoflurane-inhalation anesthesia, the animal was exsanguinated after blood collection for clinical pathology. The kidneys and other organs/tissues were fixed in 10% neutral-buffered formalin, embedded in paraffin, and sectioned. Specimens were stained with hematoxylin and eosin (HE), periodic acid-Schiff (PAS), Congo red, Masson's trichrome, or periodic acid-methenamine-silver (PAM) stains. Immunohistochemistry was performed with antibodies against IgG (goat IgG, 1:100; Jackson ImmunoResearch, West Grove, PA, USA), IgM (goat IgG, 1:200; Bethyl Laboratories, Inc., Montgomery, TX, USA), C3 (rabbit IgG, 1:500; Novus Biologicals, Littleton, CO, USA), α-SMA (mouse IgG, 1:100; Dako A/S, Glostrup, Denmark) and Ki-67 (rabbit IgG, 1:100; Abcam, Cambridge, UK) using the peroxidase-avidin-biotin complex technique with a VECTASTAIN® Elite ABC kit (Vector Laboratories Inc., Burlingame, CA, USA). Formalin-fixed tissue specimens from the kidney were examined electron microscopically. Specimens were cut into 1-mm^3 cubes, refixed in 2.5% glutaraldehyde and postfixed in 1% OsO4 for 2 hr. These specimens were then dehydrated through ascending grades

Received: 11 March 2015, Accepted: 3 August 2015
Published online in J-STAGE: 4 September 2015
*Corresponding author: K Ago (e-mail: kyouhei.agou@meiji.com)

Table 1. Hematology in an 8-week-old ICR Mouse

Parameters	Value	Historical control data
WBC ($\times 10^3/\mu L$)	3.70	4.03 ± 1.09
RBC ($\times 10^6/\mu L$)	6.33	7.75 ± 0.59
Hemoglobin (g/dL)	9.4	12.9 ± 0.9
Hematocrit (%)	29.1	41.6 ± 2.8
MCV (fL)	46.0	53.8 ± 2.0
MCH (pg)	14.8	16.6 ± 0.5
MCHC (g/dL)	32.3	30.9 ± 0.8
Platelets ($\times 10^3/\mu L$)	1398	1653 ± 200
Lymphocytes ($\times 10^3/\mu L$)	1.47	3.24 ± 0.94
Monocytes ($\times 10^3/\mu L$)	0.06	0.05 ± 0.04
Neutrophils ($\times 10^3/\mu L$)	2.11	0.61 ± 0.20
Eosinophils ($\times 10^3/\mu L$)	0.06	0.12 ± 0.05
Basophils ($\times 10^3/\mu L$)	0.00	0.00 ± 0.00
Reticulocytes ($\times 10^9/\mu L$)	492.5	400.2 ± 83.0

Historical control data are shown as the mean ± standard deviation.

Table 2. Blood Chemistry in an 8-week-old ICR Mouse

Parameters	Value	Historical control data
LDH (U/L)	357	200 ± 54
AST (U/L)	118	35 ± 5
ALT (U/L)	20	20 ± 6
ALP (U/L)	140	359 ± 93
CPK (U/L)	533	181 ± 94
Urea nitrogen (mg/dL)	139.1	19.6 ± 3.5
Creatinine (mg/dL)	0.34	0.06 ± 0.02
Ca (mg/dL)	10.1	9.6 ± 0.4
Glucose (mg/dL)	253	353 ± 62
Triglycerides (mg/dL)	59	93 ± 37
Total cholesterol (mg/dL)	286	131 ± 23
Total protein (g/dL)	4.3	4.3 ± 0.4
Albumin (g/dL)	2.3	2.5 ± 0.2
A/G	1.1	1.4 ± 0.1

Historical control data are shown as the mean ± standard deviation.

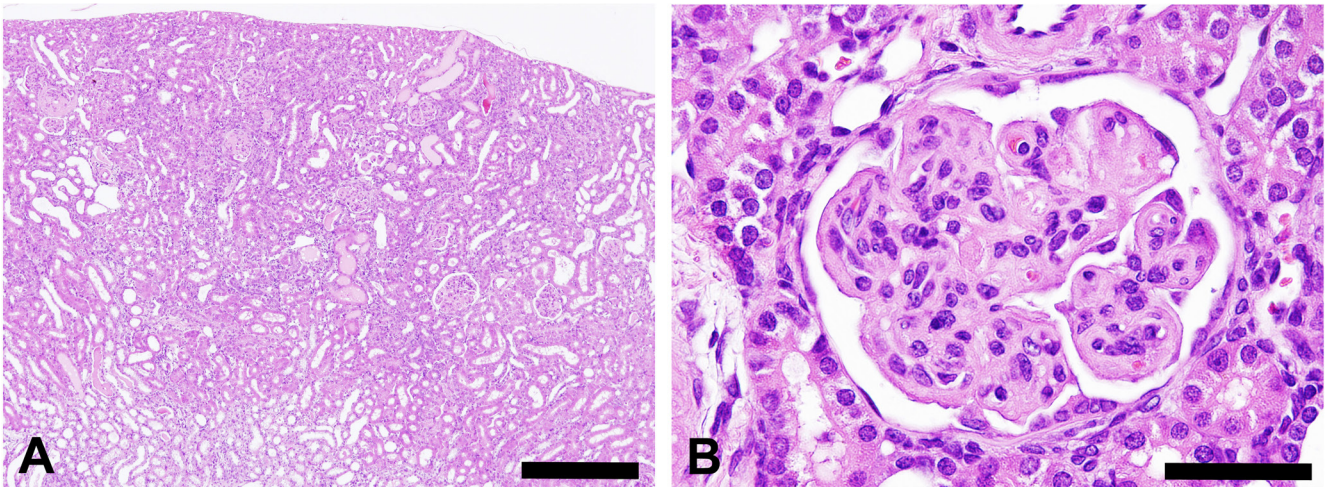

Fig. 1. Kidney of an 8-week-old ICR mouse. (A) Diffuse glomerular lesions are associated with tubular lesions, e.g., basophilic changes and hyaline casts in bilateral kidneys. Hematoxylin and eosin staining; scale bar = 400 µm. (B) A glomerulus showing thickening of capillary walls and mesangial expansion. Hematoxylin and eosin staining; scale bar = 50 µm.

of alcohol and embedded in epoxy resin. Ultrathin sections were double stained with uranyl acetate and lead citrate, and examined using a JEM 1400 transmission electron microscope (JEOL Ltd., Tokyo, Japan) at 80 kV. Blood was collected using EDTA-3K-treated and heparinized syringes for hematology and blood chemistry, respectively. Parameters of hematology (Table 1) were determined using a hematology analyzer (XT2000iV Sysmex Corporation, Kobe, Japan). Parameters of blood chemistry (Table 2) were measured in plasma using an automatic analyzer (TBA-120FR Toshiba Medical Systems, Inc., Tokyo, Japan). The data for the present case were compared with historical control data of 5- to 7-week-old mice in our laboratory.

At necropsy, pale discoloration of both kidneys was observed, but ascites and edema were not seen. There were no particular findings in the other organs or tissues examined except atrophy of the thymus. Histopathologically, diffuse glomerular changes were observed in both kidneys (Fig. 1). The glomerular changes consisted of a thickening of the capillary walls and mesangial expansion due to increased amounts of matrix (Fig. 1). Some glomeruli showed mesangial sclerotic changes, a crescent form-like thickening of Bowman's capsule and mononuclear cell infiltration. Besides lesions in the glomeruli, basophilic tubules, hyaline casts, and interstitial mononuclear cell infiltration were present. Thickened capillary walls and an expanded mesangial area were positively stained with PAS (Fig. 2) but were negative for Congo red staining. The mesangial area was stained black with PAM and blue with Masson's trichrome (Fig. 2). Thickened capillary walls showed double contouring of the basement membrane, but no spikes were seen as determined by PAM staining. Immunohistochemi-

cal analysis demonstrated that the glomerulus, principally the capillary wall, was positive for IgM and α-SMA (Fig. 3) but negative for IgG and C3. In addition, Ki-67-positive cells were observed in glomeruli (Fig. 3). The lesions in Bowman's capsules were also stained blue for Masson's trichrome and positive for Ki-67. Electron microscopic examination revealed mesangial interposition in the capillary wall and subendothelial deposition of basement membrane-like material (Fig. 4). This mesangial interposition and newly formed basement membrane-like material resulted in double contouring of the basement membrane and a thickened capillary wall. The foot processes of the podocytes were segmentally fused, and loss of endothelial fenestra was observed. Electron-dense deposits were not noted despite immunoreactivity to IgM in the thickened capillary wall. In the other tissues and organs tested, significant changes were not noted except for moderate atrophy of the cortex in the thymus. Minimal or mild lesions were observed in some organs including cardiomyopathy in the heart, anisokaryosis in the liver and atrophy of the acinar cells in the pancreas, mesenteric lymph nodes and white pulp in the spleen. Clinical pathological analysis demonstrated significant increases in blood urea nitrogen and creatinine. In addition, slight increases in AST and neutrophil counts and a decrease in erythrocytic parameters were also noted (Table 1, 2).

Amyloidosis, glomerulonephritis and glomerulosclerosis are well-known age-related spontaneous glomerular lesions in the aging ICR mouse[3]. In the present case, amyloidosis was not observed, as there were no Congo red staining deposits. In the thickened capillary wall, mesangial interposition, activation of mesangial cells and/or phenotypic changes in mesangial cells were suggested by immunoreactivity to α-SMA. Mesangial interposition was also identified in ultrastructural observation. In addition, the presence of Ki-67-positive cells suggested an increase in mesangial cells and the parietal epithelium of the Bowman's capsule. Immunoreactivity to IgM in the thickened capillary wall was suggestive of immune complex formation. However, it was not identified by the electron microscopic examination. We therefore considered the immunoreactivity to be due to exudation of plasma components in subendothelial regions. The above morphological findings and suggestive evidence of mesangial cell activation are compatible with diagnostic features of glomerulonephritis in the current INHAND[8]. Accordingly, we therefore considered the present case as most likely glomerulonephritis, which may have been spontaneous or genetically related. The present case might not have been caused by an immunological mechanism.

The cause and pathogenesis of glomerulonephritis are not completely understood. As in the case of membranoproliferative glomerulonephritis, secondary conditions including infectious diseases, rheumatologic diseases and neoplasms are more common than the primary form of disease in humans[9, 10]. In this regard, no evidence for the abovementioned diseases was detected in the present case on the basis of extrarenal histopathology and clinical pathology. Therefore, the present case was considered to be a primary case of

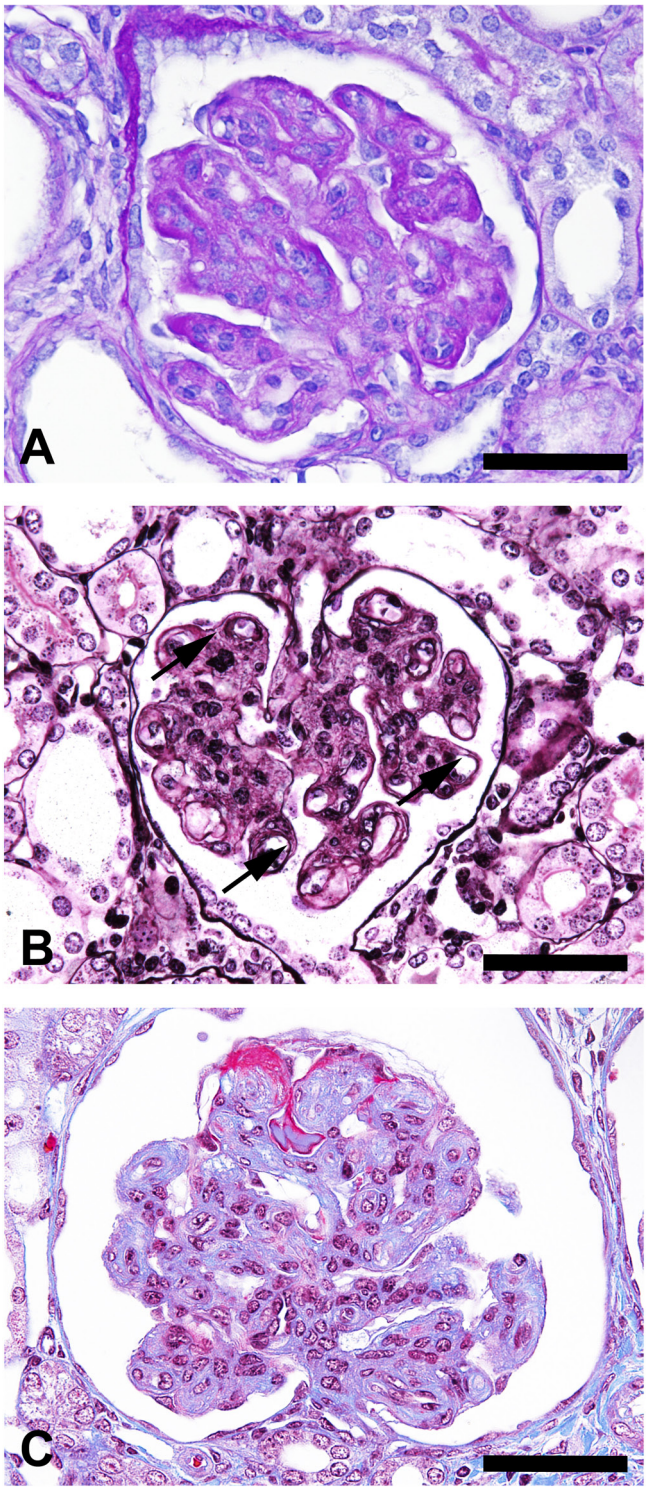

Fig. 2. Glomerulus in an 8-week-old ICR mouse. (A) The thickened capillary wall and expanded mesangial area show positive staining with PAS. Scale bar = 50 µm. (B) The thickened capillary wall shows a double-contoured basement membrane (arrows) and expanded mesangial area stained black with PAM. Scale bar = 50 µm. (C) The thickened capillary wall and expanded mesangial area are stained blue with Masson's trichrome. Scale bar = 50 µm.

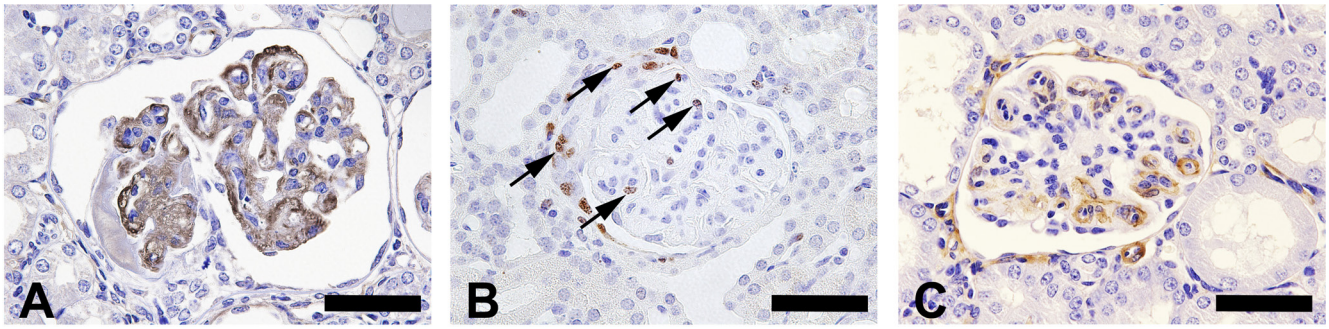

Fig. 3. Immunohistochemical staining of the glomerulus of an 8-week-old ICR mouse. (A) The thickened capillary wall and expanded mesangial area show positive staining for IgM. Scale bar = 50 µm. (B) The glomeruli and crescent show Ki-67-positive cells (arrows). Scale bar = 50 µm. (C) The thickened capillary wall show positive staining for α-SMA. Scale bar = 50 µm.

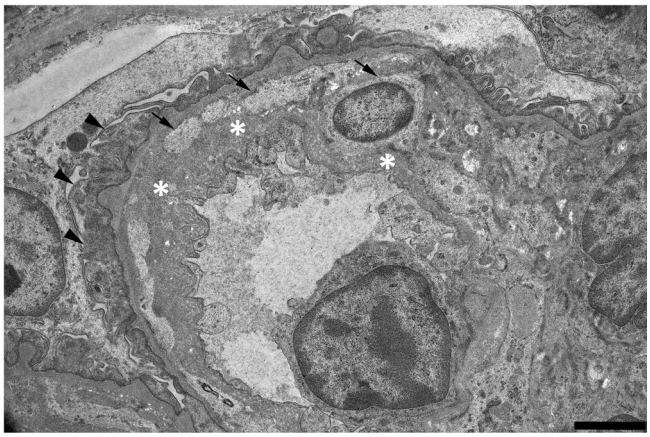

Fig. 4. Electron micrographs of glomerular capillary walls in an 8-week-old ICR mouse. The thickened capillary wall shows mesangial interposition (arrows), newly formed basement membrane-like material (asterisks) and fused podocyte foot processes (arrowheads). Scale bar = 2 µm.

glomerulonephritis.

A previous study of a 33-day-old ICR mouse indicated spontaneous idiopathic glomerulopathy and a thickening of the glomerular capillary walls with double-contoured basement membrane and enlarged mesangial area due to PAS-positive hyaline material[11], and this case was similar to the present case with regard to age, strain and morphological features. In the above case, hyaline glomerular material was negative for C3, IgG, IgM and IgA. Ultrastructurally, low electron-dense amorphous materials were observed in the subendothelial regions, basement membrane and mesangial areas. In addition, a mouse renal disease model of ICR-derived glomerulonephritis (ICGN) that exhibited spontaneous glomerulonephritis also showed a thickened basement membrane of the capillaries and enlarged mesangial area caused by the accumulation of PAS-positive material. With development of the lesion, a sign of sclerosis was noted in the affected glomeruli[12]. Electron microscopic examination revealed thickening of the basement membrane and mesangial interposition[13, 14]. Electron-dense deposits were absent or few in number, although immunoreactivity to IgG, IgM and IgA in the glomeruli was positive. The ICGN mouse is a mutant strain derived from the ICR strain, and renal disease has previously been detected in a young mouse (approximately 40 days old). So abovementioned cases of idiopathic glomerulopathy reported by Shibuya *et al*. and glomerular lesions in ICGN mice have similarities to the present case in terms of strain and age. Evidence of an increase in mesangial cells was not identified in the above cases. However, the findings of an expanded mesangial area and double-contoured basement membrane/mesangial interposition correspond to those in the present case. Ultrastructurally, deposition of non-electron-dense material was observed on the endothelial side in the present case and the case of idiopathic glomerulopathy and on the epithelial side in the case of ICGN mice. Overall, these cases have many features in common, but a difference in the location of material accumulation was detected. A mutation of the tensin2 gene was thought to be responsible for glomerulonephritis in ICGN mice[15]. Therefore, it was considered that an examination of gene mutations and further investigation are needed to clarify whether these cases have the same pathogenesis.

The etiology and incidence of the spontaneous glomerular lesions in young ICR mice remains unclear. Although further study and a greater understanding are essential for nonclinical studies of animals of this strain, we believe this case will provide useful information as the background control data of ICR mice for the toxicity studies.

Acknowledgments: The authors wish to thank Satoko Tomioka and Fumi Ito in our laboratory for their excellent technical support and scientific advice and Dr. Jerrold M. Ward for helpful comments regarding this manuscript.

Disclosure of Potential Conflicts of Interest: The authors declare that they have no conflicts of interest.

References

1. Seely JC. Kidney. In: Pathology of the Mouse: Reference and Atlas. Maronpot RR, Boorman GA, and Gaul BW (eds). Cache River Press, Vienna, 207–234. 1999.
2. Wojcinski ZW, Albassam MA, and Smith GS. Hyaline glomerulopathy in B6C3F1 mice. Toxicol Pathol. **19**: 224–229. 1991. [Medline] [CrossRef]
3. Maita K, Hirano M, Harada T, Mitsumori K, Yoshida A, Takahashi K, Nakashima N, Kitazawa T, Enomoto A, Inui K, Shirasu Y. Mortality, major cause of moribundity, and spontaneous tumors in CD-1 mice. Toxicol Pathol. **16**: 340–349. 1988. [Medline] [CrossRef]
4. Shimoda HK, Yamamoto M, Shide K, Kamezaki K, Matsuda T, Ogawa K, Harada M, and Shimoda K. Chronic thrombopoietin overexpression induces mesangioproliferative glomerulopathy in mice. Am J Hematol. **82**: 802–806. 2007. [Medline] [CrossRef]
5. Pickering MC, Cook HT, Warren J, Bygrave AE, Moss J, Walport MJ, and Botto M. Uncontrolled C3 activation causes membranoproliferative glomerulonephritis in mice deficient in complement factor H. Nat Genet. **31**: 424–428. 2002. [Medline]
6. Vernon KA, Pickering MC, and Cook T. Experimental models of membranoproliferative glomerulonephritis, including dense deposit disease. Contrib Nephrol. **169**: 198–210. 2011. [Medline] [CrossRef]
7. Cybulsky AV, Quigg RJ, and Salant DJ. Experimental membranous nephropathy redux. Am J Physiol Renal Physiol. **289**: F660–F671. 2005. [Medline] [CrossRef]
8. Frazier KS, Seely JC, Hard GC, Betton G, Burnett R, Nakatsuji S, Nishikawa A, Durchfeld-Meyer B, and Bube A. Proliferative and nonproliferative lesions of the rat and mouse urinary system. Toxicol Pathol. **40**(Suppl): 14S–86S. 2012. [Medline] [CrossRef]
9. Zhou XJ, and Silva FG. Membranoproliferative Glomerulonephritis. In: Heptinstall's Pathology of the Kidney, 6th ed. Jennette JC, Olson JL, Schwartz MM, and Silva FG (eds). Wippincott Williams & Wilkins, Philadelphia. 253–319. 2007.
10. D'Agati VD, Jennette JC, and Silva FG. Membranoproliferative Glomerulonephritis. In: Non-neoplastic Kidney Diseases Atlas of Nontumor Pathology Series No.4. D'Agati VD, Jennette JC, and Silva FG (eds). American Registry of Pathology, Washington, DC. 2005.
11. Shibuya K, Tajima M, Yamate J, and Kudow S. Idiopathic glomerulopathy in a young ICR mouse. J Comp Pathol. **103**: 107–111. 1990. [Medline] [CrossRef]
12. Ogura A, Asano T, Matsuda J, Takano K, Nakagawa M, and Fukui M. Characteristics of mutant mice (ICGN) with spontaneous renal lesions: a new model for human nephrotic syndrome. Lab Anim. **23**: 169–174. 1989. [Medline] [CrossRef]
13. Ogura A, Asano T, Matsuda J, Koura M, Nakagawa M, Kawaguchi H, and Yamaguchi Y. An electron microscopic study of glomerular lesions in hereditary nephrotic mice (ICGN strain). Virchows Arch A Pathol Anat Histopathol. **417**: 223–228. 1990. [Medline] [CrossRef]
14. Ogura A, Fujimura H, Asano T, Koura M, Naito I, and Kobayashi Y. Early ultrastructural glomerular alterations in neonatal nephrotic mice (ICGN strain). Vet Pathol. **32**: 321–323. 1995. [Medline] [CrossRef]
15. Cho AR, Uchio-Yamada K, Torigai T, Miyamoto T, Miyoshi I, Matsuda J, Kurosawa T, Kon Y, Asano A, Sasaki N, and Agui T. Deficiency of the tensin2 gene in the ICGN mouse: an animal model for congenital nephrotic syndrome. Mamm Genome. **17**: 407–416. 2006. [Medline] [CrossRef]